

# Synthesis, Crystal Structures, and Thermal Properties of Protic Metal-Containing Ionic Liquids, Diethanolammonium Halometallates: $(HOCH_2CH_2)_2NH_2FeCl_4$ and $((HOCH_2CH_2)_2NH_2)_2CoCl_4$

M. A. Zakharov<sup>a</sup>, \*<sup>a</sup>, Yu. V. Filatova<sup>a</sup>, M. A. Bykov<sup>a</sup>, N. V. Avramenko<sup>a</sup>, and L. A. Aslanov<sup>a</sup>

<sup>a</sup>*Moscow State University, Moscow, Russia*

\*e-mail: max@struct.chem.msu.ru

Received October 15, 2019; revised November 5, 2019; accepted November 15, 2019

**Abstract**—Protic metal-containing ionic liquids with the diethanolammonium cation ( $HO-CH_2-CH_2)_2NH_2^+$  (DEAH $^+$ ) and anions  $FeCl_4^-$  and  $CoCl_4^{2-}$  (DEAH $FeCl_4$  (**I**), (DEAH) $_2CoCl_4$  (**II**)) are synthesized. The crystal structures of compounds **I** and **II** are determined by X-ray structure analysis (CIF files CCDC nos. 1957208 (**I**) and 1957189 (**II**)). Compound **I** has a layered structure. The layer consists of the DEAH $^+$  cations with the disordered system of hydrogen bonds and attached  $FeCl_4^-$  anions. The structure of compound **II** represents a three-dimensional framework consisting of the DEAH $^+$  cations and  $CoCl_4^{2-}$  anions linked by hydrogen bonds. The thermal analysis shows that the melting points of compounds **I** (45°C) and **II** (55°C) are lower than 100°C, the enthalpy of melting of compound **I** is higher than that of compound **II**, and the decomposition temperature of compound **II** (210°C) is higher than that of compound **I** (128°C).

**Keywords:** metal-containing ionic liquids, protic ionic liquids, crystal structure, thermal properties

**DOI:** 10.1134/S1070328420040077

## INTRODUCTION

According to many prognoses, the global consumption of energy will significantly increase to the middle of the 21st century, and this increased demand would be satisfied in part due to the use of renewable energy sources. Since the action of solar panels is discontinuous, compatible large-scale devices of energy accumulation should be developed for power consumption in the night time. Large-capacity electrical accumulators with a high energy density made of cheap materials are needed [1].

Flow accumulators based on nonaqueous systems propose broader electrochemical windows, a higher efficiency of the charging cycle, a decreased temperature sensitivity, a prolonged service life, and even favorable cost predictions in some cases. Accumulators with ionic liquids are perspective, since they nearly do not evaporate, which fulfills the requirements of fire safety.

Ionic liquids (ILs) are intensively studied during the last three decades due to the diversity and specificity of their properties as solvents [2, 3], catalysts [2, 4], molecular magnets [5–7], electrolytes for accumulators [8, 9], and many other applications. A particular class of ILs represents salts being liquid at room tem-

perature (room temperature ionic liquids). As known, the knowledge of the structure makes it possible to reveal the dependence of the properties on the structure and composition, but the study of the structures of the liquids is associated with some difficulties [10]. The X-ray structure analysis of compounds gives incontestable advantages. Unfortunately, however, this method is inappropriate in the case of ILs, which often undergo glass transitions rather than crystallization. The salts studied in this work by X-ray diffraction analysis crystallize at the temperature lower than 100°C and, hence, can be classified as ILs.

Protic ILs found use in various fields [3, 11, 12]. Protic ILs are synthesized via the stoichiometric reaction of the Brønsted acid and Brønsted base and contain the dissociating proton in the cation (unlike traditional aprotic ILs) [3]. Metal-containing ILs (ionic liquids with the coordinated metal cation) became a new trend in the investigation of ILs [13]. Protic metal-containing ILs (PMILs) were described earlier [14].

A new group of ILs (MetIL) [15–19] containing transition metal ions as coordination sites and amino alcohols as ligands has recently been proposed. There are many interesting results related to the synthesis,

structures, and properties of MetIL with the general formula  $MA_2 \cdot 6L$ , where  $M = \text{Fe(III)}, \text{Cu(II)}, \text{Mn(II)}, \text{and Zn(II)}$ ;  $A = \text{CF}_3\text{SO}_3^- = \text{OTf}^-$  (triflate anion);  $N(\text{SO}_2\text{CF}_3)_2^- = \text{NTf}_2$  (bis(trifluoromethylsulfonyl)imide);  $\text{CH}_3(\text{CH}_2)\text{CH}(\text{C}_2\text{H}_5)\text{COO}^- = \text{EHN}$  (2-ethylhexanoate ion); and  $L = \text{DEA}$  (diethanolamine) or  $\text{EA}$  (ethanolamine). All synthesized MetIL are considered to be individual coordination compounds rather than solutions of transition metal salts or their complexes with ligand excess [15–19]. They have two advantages: a low cost and a high concentration of metals that cannot be reached in salt solutions [20, 21].

It is reported [22] on RTIL containing the  $\text{Ag}(\text{H}_2\text{N}-\text{R})_2^+$  or  $\text{Zn}(\text{H}_2\text{N}-\text{R})_4^{2+}$  cations ( $\text{R}$  is alkyl group). There is a series of ILs containing ferrocenyl-functionalized cations [23]. The synthesis, structures, and properties of  $\text{Fe}((\text{HOCH}_2\text{CH}_2)_2\text{NH})_6(\text{CF}_3\text{SO}_3)_3$  were described [24].

A series of articles on RTIL containing anions based on transition metals has recently been published. The examples represent the compounds containing imidazolium cations with tetrahedral haloferates and phosphonium cations with various cobaltates and RTIL consisting of alkylammonium, phosphonium, or imidazolium and polyoxotungstate clusters [25, 26]. The possibility of using  $\text{EmimFeCl}_4$  in accumulators was described [27]. Other fields of using ILs with the  $\text{FeCl}_4^-$  anion were described [13, 28–32].

In this work, we present the synthesis, crystal structures, and thermal properties of two protonic metal-containing ILs with the diethanolammonium cation  $(\text{HO}-\text{CH}_2-\text{CH}_2)_2\text{NH}_2^+$  and anions  $\text{FeCl}_4^-$  or  $\text{CoCl}_4^{2-}$ .

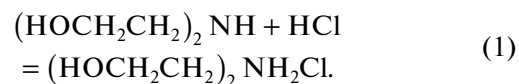
## EXPERIMENTAL

The following reagents were used:  $\text{FeCl}_3 \cdot 6\text{H}_2\text{O}$  (analytical grade),  $\text{CoCl}_2 \cdot 6\text{H}_2\text{O}$  (analytical grade),  $\text{HCl}$  (reagent grade),  $\text{H}_2\text{SO}_4$  (reagent grade),  $(\text{HOCH}_2\text{CH}_2)_2\text{NH}$  (99%, Acros),  $\text{Fe}$  (chips, reagent grade), and  $\text{P}_4\text{O}_{10}$  (high-purity grade).

**Synthesis of iron(III) chloride.** Anhydrous iron chloride was synthesized by the reaction of iron chips with dried dichlorine. Concentrated  $\text{HCl}$  (2.511 mol, 79 mL) was added by small portions from a dropping funnel to the Wurtz flask containing  $\text{KMnO}_4$  (12.5 g, 79 mmol). The reaction mixture was slightly heated. Evolved dichlorine was first passed through a washing flask filled with concentrated  $\text{H}_2\text{SO}_4$  and then over  $\text{Fe}$  chips (5 g, 89.3 mmol) placed in a dry quartz tube. The tube was heated with an industrial drier ( $T \approx 470^\circ\text{C}$ ) during the reaction. Lustrous black-brown hygro-

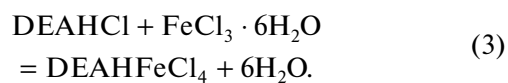
scopic crystals were obtained and sealed in glass ampules. The yield of  $\text{FeCl}_3$  was 89%.

**Synthesis of protonic ionic liquid of diethanolammonium (DEAHC).** Diethanolammonium chloride was synthesized using a described procedure [33] via the reaction



Hydrochloric acid ( $\rho = 1.111 \text{ g/cm}^3$ ,  $\omega = 22.54 \text{ wt \%}$ ) with a 5% excess of the stoichiometric amount (54.1 mL, 371 mmol) was added dropwise with stirring to a round-bottom flask containing diethanolamine (37.103 g, 353.4 mol) in dichloromethane (50 mL) with a reflux condenser placed in the bath with ice. The resulting solution was magnetically stirred for 2 h. Then the solvent was distilled from the reaction mixture on a rotary evaporator to a constant weight. As a result, a transparent viscous liquid was obtained in a yield of 96%.

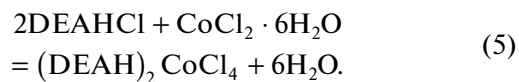
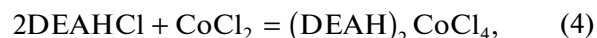
**Synthesis of diethanolammonium tetrachloroferate(III) (I)** was carried out by two methods via the reactions



In both cases, the syntheses were carried out similarly with the only difference that the weight of the  $\text{FeCl}_3$  salt was taken with allowance for water of crystallization in the case of hexahydrate, whereas the synthesis with anhydrous freshly prepared iron(III) chloride was carried out in a dry box under an argon atmosphere.

A glass bottle with a cover was loaded with  $\text{FeCl}_3$  (6.013 g, 37 mmol) or  $\text{FeCl}_3 \cdot 6\text{H}_2\text{O}$  (10.009 g, 37 mmol) and diethanolammonium chloride (5.236 g, 37 mmol). Then the mixture was magnetically stirred on heating to  $70^\circ\text{C}$  for 3 h to complete homogenization. The obtained dark brown viscous substance was placed in a desiccator with  $\text{P}_4\text{O}_{10}$ . In both cases, brown crystals of compound I were formed in 1 week.

**Synthesis of diethanolammonium tetrachlorocobaltate(II) (II)** was carried out by two methods using cobalt(II) chloride hexahydrate or anhydrous cobalt chloride via the reactions



In both cases, the syntheses were similar, but the weight of the  $\text{CoCl}_2$  salt was taken with allowance for water of crystallization in the case of hexahydrate, whereas the synthesis with anhydrous cobalt(II) chlo-

ride was carried out in a dry box under an argon atmosphere.

A glass bottle with a cover was loaded with  $\text{CoCl}_2$  (0.507 g, 3.9 mmol) or  $\text{CoCl}_2 \cdot 6\text{H}_2\text{O}$  (0.928 g, 3.9 mol) and diethanolammonium chloride (1.104 g, 7.8 mol). Then the mixture was magnetically stirred on heating to 50°C for 1 h to the complete homogenization. The obtained dark blue-violet liquid was placed in a desiccator with  $\text{P}_4\text{O}_{10}$ . In both cases, dark blue crystals of compound **II** were formed in 1 week.

The samples of the obtained metal-containing ILs were studied by differential scanning calorimetry (DSC) on a DSC-204 F1 instrument (NETZSCH). The measuring system was calibrated using the ISO 11357-1 standard according to the parameters of phase transitions of standard substances ( $\text{C}_6\text{H}_{12}$ , Hg, benzoic acid, Ga,  $\text{KNO}_3$ , In, Sn, Bi, and  $\text{CsCl}$ ; purity 99.99%). The systematic error of the temperature calibration (determined by In) was 0.1°C.

The samples were tested in standard aluminum cells ( $V = 56 \text{ mm}^3$ ,  $d = 6 \text{ mm}$ ) curled by a cover with a hole (the ratio of the surface area of the cell bottom to the surface area of the hole was ~40) in a nitrogen (special purity grade) flow (40 mL/min) with a heating rate of 5 K/min. The experimental data were processed using the Proteus Analysis package (NETZSCH) according to the ISO/CD 11358 standard.

Simultaneous thermogravimetric and mass spectrometric analyses of the thermal decomposition products were carried out for the samples of compounds **I** and **II**. The analysis was conducted on a STA-409 PC/PG instrument (NETZSCH) with a QMS 403C Aëlos quadrupole mass spectrometer (argon flow rate 30 mL/min in a range of 40–600°C and heating rate 5 K/min).

**X-ray structure analysis** of compounds **I** and **II** was carried out using a Stadi Vari Pilatus single-crystal X-ray diffractometer at 100 K. The crystal structures were solved by direct methods (SHELX-97 program [34]) and refined by full-matrix least squares. All atoms, except for hydrogen atoms, were refined anisotropically (SHELXL program implemented into the SHELX-97 program package [34]). The hydrogen atoms of the methylene groups were specified geometrically and were not refined. The positions of the hydrogen atoms of the OH and  $\text{NH}_2^+$  groups were revealed from the difference Fourier syntheses and refined in the isotropic approximation, where the hydrogen atoms of the hydroxyl groups were refined with the fixed O–H distance equal to 0.86 Å (DFIX command). In the structure of compound **I**, two electron density peaks were found near the O(1) and O(2) oxygen atoms of the hydroxyl groups, and they were specified as hydrogen atoms with a population of 0.5, which were refined as indicated above. The WinGX program [35] was used for data processing. The struc-

tures were drawn using the Diamond 3.0 program [36]. The crystallographic data and detection details are presented in Table 1.

The crystal structures were deposited with the Cambridge Crystallographic Data Centre (CIF files CCDC nos. 1957208 (**I**) and 1957189 (**II**); deposit@ccdc.cam.ac.uk or [http://www.ccdc.cam.ac.uk/data\\_request/cif](http://www.ccdc.cam.ac.uk/data_request/cif)). The parameters of the crystal structures of compounds **I** and **II** are also available from the authors.

## RESULTS AND DISCUSSION

The independent part of the unit cell in the structure of compound **I** consists of the  $\text{DEAH}^+$  cation and  $\text{FeCl}_4^-$  anion. The iron atom is surrounded by the chloride ions at the vertices of a distorted tetrahedron (Fig. 1) with the  $\text{Fe}(1)\text{--Cl}(1)$  (2.1663(15) Å),  $\text{Fe}(1)\text{--Cl}(2)$  (2.2096(14) Å),  $\text{Fe}(1)\text{--Cl}(3)$  (2.1710(14) Å), and  $\text{Fe}(1)\text{--Cl}(4)$  (2.1902(15) Å) distances. The chlorine atoms forming hydrogen bonds with the nitrogen atoms of diethanolammonium ( $\text{N}(1)\cdots\text{Cl}(2)$  3.468(5),  $\text{N}(1)\cdots\text{Cl}(2')$  3.517(5), and  $\text{N}(1)\cdots\text{Cl}(4)$  3.338(5) Å) are remote from the iron atom at the longest distance. The hydrogen atoms of the hydroxyl groups were refined in two equally populated (0.5 each) positions, since, on the one hand, the O(2) and O(1) atoms form two short distances each (2.758(6) and 2.719(5) Å) suitable for hydrogen bonding. On the other hand, the electron density peaks suitable for hydrogen atoms are localized from the difference Fourier synthesis. The cations form tetramers by hydrogen bonds between the O(2) and O(1) atoms of different diethanolammonium molecules, and the assumed disordering of the hydrogen atoms over two positions can be explained by the equally probable formation of hydrogen bonds either via the H(2) and H(4) atoms (hydrogen bonds are shown by dashed lines in Fig. 2), or via the H(1) and H(3) atoms (hydrogen bonds are shown by dotted lines in Fig. 2).

The tetramers form crimped layers perpendicular to the *a* axis. The anions supplement the layers of the cations by ionic interactions and hydrogen bonds ( $\text{N}(1)\cdots\text{Cl}(2)$  3.468(5),  $\text{N}(1)\cdots\text{Cl}(2')$  3.517(5), and  $\text{N}(1)\cdots\text{Cl}(4)$  3.338(5) Å). The van der Waals forces act between the layers (Fig. 3).

The independent part of the unit cell of the structure of compound **II** consists of one  $\text{DEAH}^+$  cation and halved  $\text{CoCl}_4^{2-}$  anion (the cobalt atom lies on the two-fold axis) (Fig. 4). The cobalt atom has the coordination environment of the chlorine atoms at the vertices of a distorted tetrahedron (Fig. 4). The Co–Cl distances in the  $\text{CoCl}_4$  tetrahedron are equal to 2.2842(7) and 2.2723(7) Å for Co–Cl(1) and Co–Cl(2), respectively. The anions form layers perpendicular to the *c* axis. The cations are linked to each other by hydrogen bonds between the nitrogen atoms

**Table 1.** Crystallographic data and detection conditions for the samples of compounds **I** and **II**

| Parameter  | Value                  |                         |
|--|------------------------|-------------------------|
|  | <b>I</b>               | <b>II</b>               |
| Empirical formula  | $C_4H_8NO_2Cl_4Fe$     | $C_8H_{16}N_2O_4Cl_4Co$ |
| $FW$   | 303.8                  | 413                     |
| Radiation; $\lambda$ , Å                                 | $CuK_\alpha$ (1.54186) | $MoK_\alpha$ (0.71073)  |
| Crystal system   | Monoclinic             | Monoclinic              |
| Space group  | $P2_1/c$               | $C2/c$                  |
| $a$ , Å  | 7.781(1)               | 11.4866(9)              |
| $b$ , Å  | 12.764(1)              | 9.2475(6)               |
| $c$ , Å  | 11.947(1)              | 17.164(1)               |
| $\beta$ , deg  | 90.77(1)               | 108.273(6)              |
| $V$ , Å <sup>3</sup>                                     | 1186.4(2)              | 1731.3(2)               |
| $Z$  | 4                      | 4                       |
| $\rho_{\text{calc}}$ , g/cm <sup>3</sup>                 | 1.701                  | 1.585                   |
| Temperature, K   | 293(2)                 | 293(2)                  |
| $\mu$ , mm <sup>-1</sup>                                 | 18.242                 | 1.617                   |
| $F(000)$   | 612                    | 852                     |
| Range of $\theta$ , deg                                  | 5.07–66.40             | 2.499–31.092            |
| Total number of reflections                              | 7154                   | 12523                   |
| Number of independent reflections ( $R_{\text{int}}$ )   | 2011 (0.0849)          | 2748 (0.1141)           |
| Number of reflections with $I > 2\sigma(I)$              | 1036                   | 2052                    |
| Number of refined parameters                             | 125                    | 104                     |
| GOOF for $F^2$   | 0.785                  | 1.018                   |
| $R_1$ for $I > 2\sigma(I)$                               | 0.0382                 | 0.0437                  |
| $wR_2$ (for all data)                                    | 0.0652                 | 0.1335                  |
| Residual electron density (min/max), $e\text{ \AA}^{-3}$ | –0.21/0.24             | –0.71/1.42              |

of the amino groups and the oxygen atoms of the hydroxyl groups ( $N(1)\cdots O(1)$  2.799(3),  $N(1)\cdots O(2)$  2.808(4) Å) to form chains of the cations extended along the [110] direction (Fig. 5). The adjacent cationic chains are linked to each other by the symmetry axes 2 and  $2_1$  and are joined by the anions via hydrogen bonds between the oxygen atoms of the hydroxyl group and chlorine atoms ( $O(2)\cdots Cl(2)$  3.079(3),  $O(1)\cdots Cl(1)$  3.129(2) Å) into a three-dimensional framework (Fig. 6).

The DSC results for all synthesized metal-containing ILs are presented in Table 2. The difference in melting points of compounds **I** and **II** possibly depends on the differences in the crystal structures and IL compositions: the crystal structure of compound **I** is layered with the interaction between the layers via the van der Waals forces, whereas

the structure of compound **II** represents a three-dimensional framework formed by the Coulomb interactions between the cations and anions and  $O\cdots H\cdots O$  and  $N\cdots H\cdots Cl$  hydrogen bonds. According to our data, when the hydrogen atom in the OH group of diethanolammonium is replaced by a hydrocarbon radical (e.g., methyl), the ILs undergo only the glass transitions and softening processes, whereas melting and crystallization are absent.

According to the thermal analysis (DSC–TG) data, the decomposition temperature of IL **I** was 128°C, and that of IL **II** was 210°C. The latter IL is more promising for the use due to the higher decomposition temperature.

The following can be concluded: (1) two protic metal-containing ILs were synthesized for the first time; (2) the crystal structures of the synthesized ILs

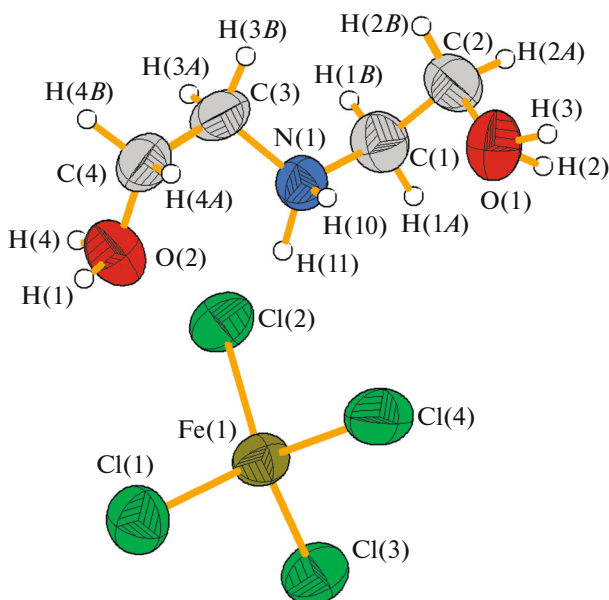


**Fig. 1.** Fragment of the structure of compound I. Thermal ellipsoids of 50% probability. The H(1), H(2), H(3), and H(4) hydrogen atoms have the population 0.5.

were determined, the structure of  $\text{DEAHFeCl}_4$  (**I**) is layered, the layer contains a layer of the  $\text{DEAH}^+$  cations with the disordered system of hydrogen bonds and attached  $\text{FeCl}_4^-$  anions, and the structure of  $(\text{DEAH})_2\text{CoCl}_4$  (**II**) represents a three-dimensional framework consisting of chains of the  $\text{DEAH}^+$  cations

linked by the anions via hydrogen bonds; and (3) the melting points of compounds **I** ( $45^\circ\text{C}$ ) and **II** ( $55^\circ\text{C}$ ) are lower than  $100^\circ\text{C}$ , the enthalpy of melting of compound **I** is higher than that of compound **II**, and the decomposition temperature of compound **II** ( $210^\circ\text{C}$ ) is higher than that of compound **I** ( $128^\circ\text{C}$ ).

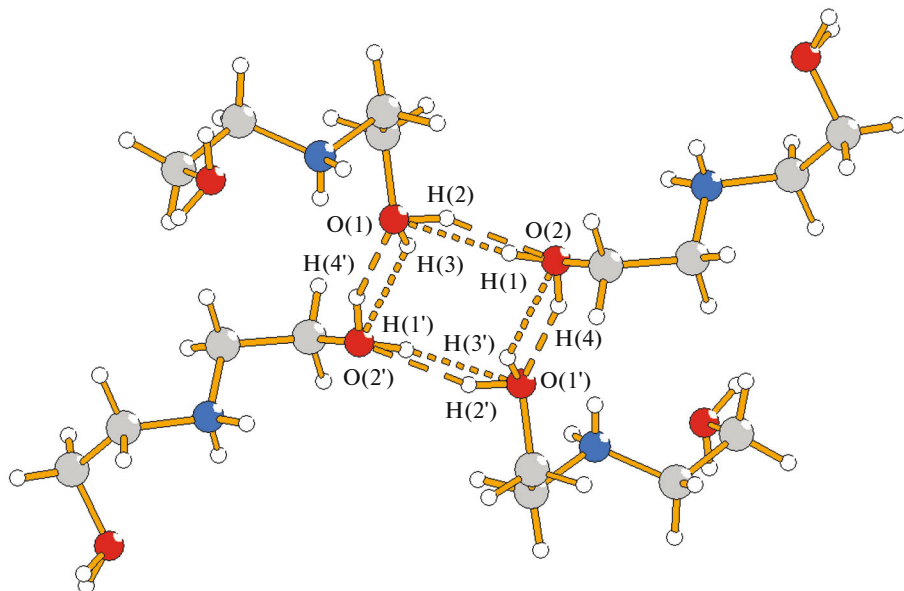


**Fig. 2.** Tetramers of the  $\text{DEAH}^+$  cations in the structure of compound I. Anions are omitted. One variant of the system of hydrogen bonds is shown by dashed lines, and another equally probable variant is shown by dotted lines.

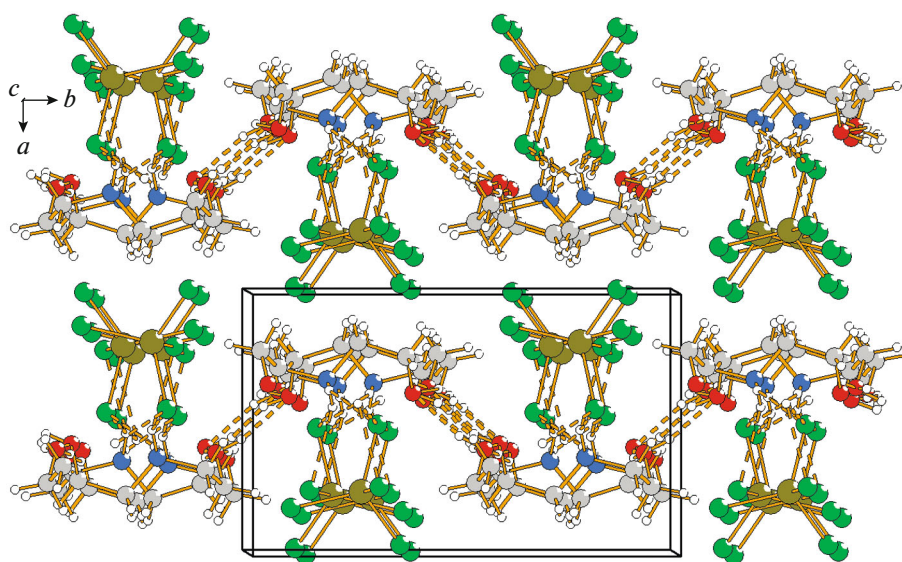


Fig. 3. Layered structure of compound I. Hydrogen bonds are shown by dashed lines. View along the  $c$  axis.

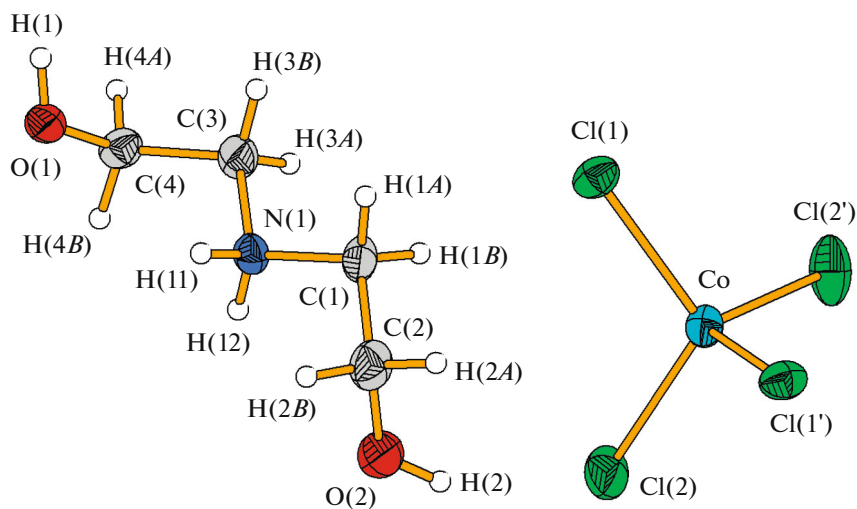
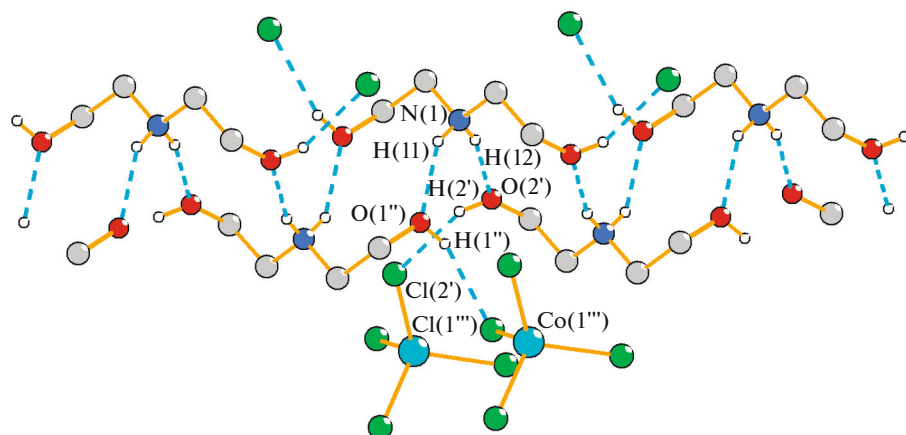


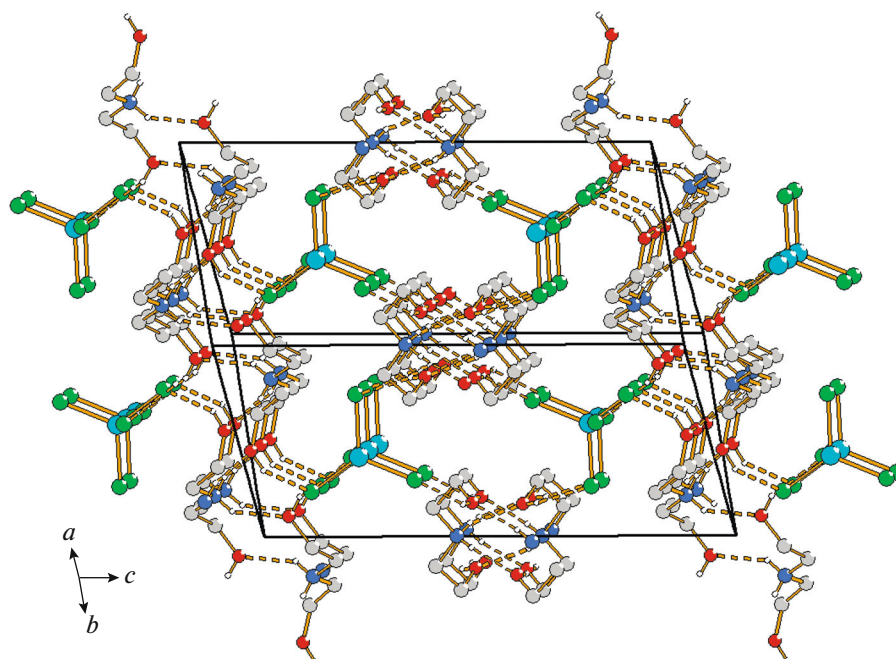
Fig. 4. Fragment of the structure of compound II. Thermal ellipsoids of 50% probability.

Table 2. DSC results for the metal-containing ionic liquids

| Sample   | $T_m$ , °C | $\Delta H_m$ , kJ/mol |
|--|------------|-----------------------|
| DEAHFeCl <sub>4</sub> (reaction (2))                 | 45.5       | 87.010                |
| DEAHFeCl <sub>4</sub> (reaction (3))                 | 45.4       | 98.308                |
| (DEAH) <sub>2</sub> CoCl <sub>4</sub> (reaction (4)) | 52.5       | 28.877                |
| (DEAH) <sub>2</sub> CoCl <sub>4</sub> (reaction (5)) | 58.2       | 34.872                |



**Fig. 5.** Chains of the  $\text{DEAH}^+$  cations in the structure of compound **II**. The anions and methylenic hydrogen atoms are omitted for clarity.



**Fig. 6.** Structure of compound **II**. Hydrogen bonds are shown by dashed lines. The hydrogen atoms of the methylene groups are omitted for clarity.

#### FUNDING

This work was supported by the Russian Foundation for Basic Research, project no. 19-08-00672a.

#### CONFLICT OF INTEREST

The authors declare that they have no conflicts of interest.

#### SUPPLEMENTARY MATERIALS

Supplementary materials are available for this article at <https://doi.org/10.1134/S1070328420040077> and are accessible for authorized users.

#### REFERENCES

1. Staiger, C.L., Pratt, H.D., III, Leonard, J.C., et al., *Proc. EESAT (16–19 Oct. 2011)*, San Diego, 2011, p. 91.
2. Vekariya, R.L., *J. Mol. Liq.*, 2017, vol. 227, p. 44.
3. Greaves, T.L. and Drummond, C.J., *Chem. Rev.*, 2015, vol. 115, p. 11379.
4. Dai, C., Zhang, J., Huang, C., and Lei, Z., *Chem. Rev.*, 2017, vol. 117, p. 6929.
5. Yoshida, Y., Tanaka, H., Saito, G., et al., *Inorg. Chem.*, 2009, vol. 48, p. 9989.
6. Yoshida, Y. and Saito, G., *J. Mater. Chem.*, 2006, vol. 16, p. 1254.

7. Hayashi, S. and Hamaguchi, H.-O., *Chem. Lett.*, 2004, vol. 33, p. 1590.
8. Hapiot, P. and Lagrost, C., *Chem. Rev.*, 2008, vol. 108, p. 2238.
9. Watanabe, M., Thomas, M.L., Zhang, S., et al., *Chem. Rev.*, 2017, vol. 117, p. 7190.
10. Hayes, R., Warr, G.G., and Atkin, R., *Chem. Rev.*, 2015, vol. 115, p. 6357.
11. Hu, J., Ma, J., Zhu, Q., et al., *Angew. Chem., Int. Ed. Engl.*, 2015, vol. 54, p. 5399.
12. Hunt, P.A., Ashworth, C.R., and Matthews, R.P., *Chem. Soc. Rev.*, 2015, vol. 44, p. 1257.
13. Zazybin, A., Rafikova, K.H., Yu, V., et al., *Russ. Chem. Rev.*, 2017, vol. 86, p. 1254.
14. Dengler, J.E., Dorodian, A., and Bernhard, R., *J. Organomet. Chem.*, 2011, vol. 696, p. 3831.
15. Anderson, T.M., Ingersoll, D., Rose, A.J., et al., *Dalton Trans.*, 2010, vol. 39, p. 8609.
16. Pratt, H.D., III, Rose, A.J., Staiger, C.L., et al., *Dalton Trans.*, 2011, vol. 40, p. 11396.
17. Pratt, H.D., III, Leonard, J.C., Steele, L.A.M., et al., *Inorg. Chim. Acta*, 2013, vol. 396, p. 78.
18. Pratt III, H.D., Ingersoll, D., Hudak, N.S., et al., *J. Electroanal. Chem.*, 2013, vol. 704, p. 153.
19. Zakharov, M.A., Fetisov, G.V., Veligzhanin, A.A., et al., *Dalton Trans.*, 2015, vol. 44, p. 18576.
20. Schaltin, S., Brooks, N.R., Binnemans, K., and Fransaer, J., *J. Electrochem. Soc.*, 2011, vol. 158, p. D21.
21. Brooks, N.R., Schaltin, S., van Hecke, K., et al., *Chem.-Eur. J.*, 2011, vol. 17, p. 5054.
22. Huang, J.-F., Luo, H., and Dai, S., *J. Electrochem. Soc.*, 2006, vol. 153, p. J9.
23. Balasubramanian, R., Wang, W., and Murray, R.W., *J. Am. Chem. Soc.*, 2006, vol. 128, p. 9994.
24. Anderson, T.M., Ingersoll, D., Rose, A.J., et al., *Dalton Trans.*, 2010, vol. 39, p. 8609.
25. Yoshida, Y., Tanaka, H., Saito, G., et al., *Inorg. Chem.*, 2009, vol. 48, p. 9989.
26. Ortiz-Acosta, D., Purdy, G.M., Scott, B., et al., *ECS Trans.*, 2009, vol. 16, p. 171.
27. Katayama, Y., Konishiike, I., Miura, T., and Kishi, T., *J. Power Sources*, 2002, vol. 109, p. 327.
28. Wang, J., Yao, H., Nie, Y., et al., *J. Mol. Liq.*, 2012, vol. 169, p. 152.
29. Sun, X., Zhao, S., and Zhang, M., *Petrol. Sci.*, 2005, vol. 2, p. 77.
30. Small, L.J., Pratt, H.D., III, Staiger, C.L., and Anderson, T.M., *Adv. Sustain. Syst.*, 2017, vol. 1, no. 1700066.
31. Estager, J., Holbrey, J.D., and Swadzba-Kwasny, M., *Chem. Soc. Rev.*, 2014, vol. 43, p. 847.
32. Wang, L.-J. and Lin, C.-H., *Mini-Rev. Org. Chem.*, 2012, vol. 9, p. 223.
33. Petrović, Z.D., Hadjipavlou-Litina, D., Pontiki, E., et al., *Bioorg. Chem.*, 2009, vol. 37, p. 162.
34. Sheldrick, G.M., *Acta Crystallogr., Sect. A: Found. Crystallogr.*, 2008, vol. 64, p. 112.
35. Farrugia, L.J., *J. Appl. Crystallogr.*, 1999, vol. 32, p. 837.
36. *Diamond. Crystal and Molecular Structure Visualization*, Bonn: Crystal Impact, 2014.

Translated by E. Yablonskaya